Development 133, 2243-2252 (2006) doi:10.1242/dev.02379

Robo1 regulates the development of major axon tracts and interneuron migration in the forebrain

William Andrews[1,2,*], Anastasia Liapi[1,*], Céline Plachez[3,*], Laura Camurri[2], Jiangyang Zhang[4], Susumu Mori[4,5], Fujio Murakami[6], John G. Parnavelas[1], Vasi Sundaresan[7,†] and Linda J. Richards[3,8,†]

The Slit genes encode secreted ligands that regulate axon branching, commissural axon pathfinding and neuronal migration. The principal identified receptor for Slit is Robo (Roundabout in *Drosophila*). To investigate Slit signalling in forebrain development, we generated Robo1 knockout mice by targeted deletion of exon 5 of the Robo1 gene. Homozygote knockout mice died at birth, but prenatally displayed major defects in axon pathfinding and cortical interneuron migration. Axon pathfinding defects included dysgenesis of the corpus callosum and hippocampal commissure, and abnormalities in corticothalamic and thalamocortical targeting. Slit2 and Slit1/2 double mutants display malformations in callosal development, and in corticothalamic and thalamocortical targeting, as well as optic tract defects. In these animals, corticothalamic axons form large fasciculated bundles that aberrantly cross the midline at the level of the hippocampal and anterior commissures, and more caudally at the medial preoptic area. Such phenotypes of corticothalamic targeting were not observed in Robo1 knockout mice but, instead, both corticothalamic and thalamocortical axons aberrantly arrived at their respective targets at least 1 day earlier than controls. By contrast, in Slit mutants, fewer thalamic axons actually arrive in the cortex during development. Finally, significantly more interneurons (up to twice as many at E12.5 and E15.5) migrated into the cortex of *Robo1* knockout mice, particularly in both rostral and parietal regions, but not caudal cortex. These results indicate that *Robo1* mutants have distinct phenotypes, some of which are different from those described in Slit mutants, suggesting that additional ligands, receptors or receptor partners are likely to be involved in Slit/Robo signalling.

KEY WORDS: Thalamocortical axons, Corpus callosum, Hippocampal commissure, Axon guidance, Cell migration, Slit, Mouse

INTRODUCTION

The CNS midline plays an important role in guiding commissural projections. The chemorepulsive ligand Slit and its receptors of the Robo family are expressed in the developing and adult brain (Yuan et al., 1999; Marillat et al., 2002) and are crucially involved in the formation of midline commissures (Kidd et al., 1998a; Kidd et al., 1998b; Brose et al., 1999; Plump et al., 2002; Bagri et al., 2002; Long et al., 2004; Sabatier et al., 2004).

In the *Drosophila* nerve cord and in the mammalian spinal cord, Robo (Roundabout in *Drosophila*) protein expression is upregulated after midline crossing, when commissural growth cones become highly responsive to Slit, preventing them from re-crossing the midline (Kidd et al., 1998a; Kidd et al., 1998b; Zou et al., 2000; Long et al., 2004; Sabatier et al., 2004). However, brain commissural and decussating axons, including the corpus callosum, optic chiasm and the corticospinal tract express Robo protein (Sundaresan et al., 2004), and respond to Slit2 both before and after they cross the midline (Plump et al., 2002; Bagri et al., 2002; Shu et al., 2003a). Thus, Slit2 may serve a different role than that observed in flies or at the midline of the spinal cord, probably because brain commissural axons grow away from the midline after they cross it, rather than remaining in close proximity to the midline as spinal commissural axons do.

Slit2 and *Slit1/2* double knockout animals display defects in corticothalamic and thalamocortical targeting, callosal and hippocampal commissure projections (Bagri et al., 2002), and defects in the formation of the optic chiasm (Plump et al., 2002). In these mice, large ectopic commissures are formed at the midline from corticothalamic axons that would not normally cross the midline. These data suggest that the Slits normally prevent these axons from crossing the midline and instead guide them to their respective targets in the thalamus.

In addition to regulating commissural axon guidance and axonal branching (Wang et al., 1999; Ozdinler and Erzurumlu, 2002; Sang et al., 2002), Slit/Robo signalling also regulates cellular migration (Hu, 1999; Wu et al., 1999; Zhu et al., 1999). Slit secreted from the ventricular zone of the lateral ganglionic eminence (LGE) repels cortical interneurons from the subventricular zone of LGE explants and inhibits tangential migration when added locally at the corticostriatal boundary of brain slices (Zhu et al., 1999). However, tangential migration was reported to take place normally in *Slit1/Slit2* double knockout mice, while the ganglionic eminence (GE) retained its repulsive activity (Marín et al., 2003).

In order to examine Slit signalling and its involvement in axonal guidance and neuronal migration, we have generated Robo1 knockout mice by targeted deletion. Here, we analyse the migration of interneurons into the neocortex and the formation of the corpus callosum, hippocampal commissure, corticothalamic and thalamocortical projections. The results reveal striking differences between the phenotypes of Robo1 and Slit knockouts, and suggest that additional mechanisms are involved in Slit/Robo signalling in these systems.

[1]Department of Anatomy and Developmental Biology, University College London, London WC1E 6BT, UK. [2]MRC Centre for Developmental Neurobiology, King's College London, London SE1 1UL, UK. [3]The University of Maryland School of Medicine, Department of Anatomy and Neurobiology, and The Program in Neuroscience, Baltimore, MD 21201, USA. [4]Johns Hopkins University School of Medicine, Department of Radiology, Division of NMR Research and Department of Biomedical Engineering, Baltimore, MD 21205, USA. [5]F. M. Kirby Research Center for Functional Brain Imaging, Kennedy Krieger Institute, Baltimore, MD 21205, USA. [6]Osaka University, Osaka, Japan. [7]Department of Cellular Pathology, St Margarets Hospital, The Plain, Epping CM16 6TN, UK. [8]The University of Queensland, School of Biomedical Sciences and The Queensland Brain Institute, Brisbane, Queensland, Australia.

*These authors contributed equally to this work
[†]Authors for correspondence (e-mail richards@uq.edu.au and vasi.sundaresan@kcl.ac.uk)

Accepted 23 March 2006

MATERIALS AND METHODS

Generation and characterization of *Robo1* knockout mice

A description of the generation of the *Robo1* knockout mice can be found in the Results section and the legend to Fig. 1. Mice were genotyped by polymerase chain reaction (PCR) using the following primers: M1510F (5′-CGAGGARGAAARSTSATGATC-3′) and 216R (5′-CCACAAGAC-TTGTGACAATACC-3′). For reverse transcriptase (RT)-PCR, primers 1510F and 200R (5′-CCTCTCTTCCAAAAGATAGCTGG-3′) were employed. Total RNA was extracted from tissue using Trizol (Invitrogen, UK) and the RT reaction was performed with either oligo dT or random primers to specifically amplify between exons 4 and 7.

Whole mount in situ hybridization for Robo1 was performed on embryonic day (E)12.5 intact mouse embryos using a modified protocol (Wilkinson, 1992; Henrique et al., 1995) as described by Camurri et al. (Camurri et al., 2004). To assess protein expression in the Robo1 knockouts, gel-electrophoresis and immunoblotting were performed as previously described (Hivert et al., 2002). Robo1 was detected using a rabbit polyclonal antibody (205) raised against the C-terminal peptide of DUTT1/ROBO1 (Xian et al., 2001). To demonstrate equivocal loading, blots were re-probed using a mouse monoclonal antibody raised against β-actin (Jackson Laboratories, MN).

Diffusion tensor magnetic resonance (DTMRI) imaging

Imaging was performed using a General Electric Omega 400 (9.4 Tesla) NMR spectrometer. A custom-made solenoid volume coil was used as the radio frequency signal transmitter and receiver. Brains were placed in home-built MR-compatible tubes filled with fomblin (Fomblin Profludropolyether, Ausimont, NJ) to prevent dehydration. Diffusion-weighted images were acquired with a 3D diffusion weighted multiple echo sequence (Mori and van Zijl, 1998). The imaging field of view was $11 \times 7.5 \times 7.5$ mm^3. The imaging matrix had a dimension of $128 \times 70 \times 72$. The spectral data were apodized by a 10% trapezoidal function and then zero-filled to $256 \times 140 \times 144$. The pixel size after the zero-filling was $43 \times 53.5 \times 52.1$ μm^3. Eight diffusion-weighted images with different diffusion gradient direction and magnitude were acquired for each sample. A repetition time of 900 ms, an echo time of 37 ms and two signal averages were used for a total imaging time of ~28-30 hours.

The diffusion tensor was calculated using a multivariate linear fitting method, and three pairs of eigenvalues and eigenvectors were calculated for each pixel. The eigenvector associated with the largest eigenvalue was referred to as the primary eigenvector. For the quantification of anisotropy, a linear measure (CL) was used (Westin et al., 2002). Using the primary eigenvector and CL, colour maps were calculated and the red, green and blue values of each pixel were defined by the orientation of its primary eigenvector with the intensity proportional to the CL. Red was assigned to the fibre orientation along the anteroposterior axis, green to the right-left axis and blue to the dorsoventral axis.

Immunohistochemistry

Brains were collected between E12.5 and E18.5. Embryos were either fixed by immersion in 4% paraformaldehyde (PFA) or transcardially perfused with saline, followed by 4% PFA, and then postfixed in the same fixative solution overnight. Brains were blocked in 3% agar and cut at 40 μm on a Vibratome (Leica) or 30 μm on a cryostat (Bright). Sections were washed in 1× phosphate buffered saline (PBS), blocked in a solution of 2% serum (v/v) and 0.2% Triton X-100 (v/v) (Sigma) in PBS for 2 hours. Normal goat serum (S-1000, Vector Laboratories, Burlingame, CA) or normal donkey serum (017-000-121, Jackson ImmunoResearch Laboratory, West Grove, PA) was used for primary antibodies made in rabbit or rat, respectively. Sections were incubated in either rabbit anti-GFAP (1:30,000; Z0334, Dako, Glostrup, Denmark); rabbit anti-neurofilament M C-terminal (1:75,000; AB1987, Chemicon, Temecula, CA); rat anti-L1 (1:5000; MAB5272, Chemicon); rabbit anti-calbindin (1:10000; D-28K, Swant, Bellinzona, Switzerland); mouse anti-GAD65 (1:200 Affinity Research Products, Exeter, UK); or rabbit anti-Robo1 or -Robo2 (1:10,000 and 1:5,000, respectively; antibodies prepared by Dr Murakami) overnight. Sections were washed in PBS and incubated in biotinylated goat anti-rabbit (1:500; Vector Laboratories) or biotinylated donkey anti-rat (1:500; Jackson ImmunoResearch Laboratory) for 2 hours, then incubated in avidin-biotin solution (1:500; Vector Laboratories) and processed as previously described (Shu et al., 2000).

Quantification of interneuron distribution

Calbindin-positive cells were counted in 200 μm coronal strips of dorsomedial neocortex at different levels along the rostrocaudal extent of the cortex at E18.5 (eight sections at each level from each of three animals for each condition). In all counts, the experimenter did not know the condition of the animal. Strips were longitudinally divided into six equal bins/sectors, from bin 1 (ventricular zone) to bin 6 (marginal zone). Interneuron migration was assessed at E12.5 by counting the total number of calbindin-positive cells that had crossed the corticostriatal notch and entered the cortex.

Carbocyanine dye tracing

Injections were made using fine-tipped glass pipettes (1-5 μl, Dummond Scientific Company, Broomall, PA) attached to a pressure injector (Picospritzer, Parker Instrumentation, NJ). Pipettes were filled with solutions of either 10% DiI or DiA (D-282 and D3883, Molecular Probes) in dimethylformamide (data shown in Fig. 5). Other brains (data shown in Fig. 7) were labelled by placing a single crystal of either DiI or DiA in the brain as previously described (Métin and Godement, 1996; Molnár et al., 1998). DiA crystals were placed in the presumptive somatosensory cortex to label corticofugal axons, and DiI crystals were placed in the dorsal thalamus to label thalamocortical axons. To label the corpus callosum and the hippocampal commissure, injections were first made into the cingulate cortex (DiI) and then the brains were cut coronally at the level of the hippocampus to allow the injection of DiA directly into the dentate gyrus. Labelled brains were stored at 37°C in darkness for 2-6 weeks and then blocked in 4% agarose and cut at either 40 μm or 100 μm using a Vibratome (40 μm sections were cut on Leica Vibratome and 100 μm sections were cut on a Vibroslice, Campden Instruments). Injection sites were verified after sectioning by the presence of a fluorescent bolus and a pipette track. Sections were washed and incubated overnight with 4′-6-Diamidino-2-Phenyllindole (DAPI, 1:20,000; D-9542, Sigma) in PBS or bisbenzimide (10 minutes in 2.5 μg/ml solution in PBS, Sigma). Images were collected using a confocal microscope (Fluoview FV5000 Olympus, NY or Leica, Microsystems, UK). Sequential images collected with the Leica microscope were subsequently reconstructed using Metamorph imaging software (Universal Imaging Corporation).

Dissociated cell cultures

Dissociated cell cultures were derived from E15 mouse telencephalons according to the method of Cavanagh et al. (Cavanagh et al., 1997). Briefly, GEs were dissected out from embryonic forebrains in Hanks' solution under a stereo microscope, and isolated tissue was dissociated enzymatically in Neurobasal media with trypsin (0.1%) and DNase I (0.001%) for 15 minutes at 37°C. Trypsin was inactivated by 10% foetal calf serum (FCS) in Neurobasal media for 5 minutes and cells dissociated by delicate tritiation with a sterile pipette tip. The resulting suspension was centrifuged at 1000 ***g*** for 3 minutes, the supernatant discarded and cells resuspended in Neurobasal media containing B27 Supplement, 100 μg/ml penicillin/streptomycin and 2 mM L-glutamine. They were then plated at a density of 2×10^5 cells on poly-L-lysine (10 μg/ml) and laminin (5 μg/ml) coated 13 mm coverslips in 24-well plates. Cultures plated were kept in a humidified incubator (95% Air/5%CO_2) at 37°C and cells were allowed to attach to the coverslips for 30 minutes. Fresh medium was then added, and again on the following morning.

RESULTS

Generation of Robo1 knockout mice

To evaluate the role of Robo1 in forebrain development, we first generated Robo1 knockout mice. In this procedure, we floxed one of a pair of exons coding for the immunoglobulin domain Ig 3a to generate a frame shift mutation. We expected a stop codon downstream and, consequently, nonsense mRNA message decay leading to a 'null' phenotype (Li and Wilkinson, 1998). To achieve this, a targeting vector was generated using a 9.9 kb genomic

fragment identified from a mouse bacterial artificial chromosome which encompasses exons 4 to 6 of Robo1 (Fig. 1A). Exon 5 was floxed with a neomycin resistance gene (positive selection) cassette at the 3′ end of exon 5, and a thymidine kinase cassette (for negative selection) was cloned into the vector arm. 129sv-derived ES were targeted and clones selected and analysed for homologous recombination by Southern blotting (Fig. 1B). Three independent clones demonstrating homologous recombination were propagated and then injected into C57Bl/6 derived blastocysts and chimeras generated. Two independently derived chimeras that had transmitted the recombinant allele were mated with Actin Cre mice (obtained from Dr D. Acampora, Kings College London) to generate founder mice where the exon5/neo cassette had been excised. These animals were bred onto a C57Bl/6 background and the resulting heterozygotes were crossed to generate homozygous deficient mice.

Southern blotting and PCR analysis of E14.5 pup DNA/RNA demonstrated that exon 5 and the neo cassette had been deleted (Fig. 1B-D), and sequence information showed that a frame shift had occurred in mice carrying the deleted allele (Fig. 1E). We predicted that the altered RNA species would undergo nonsense message decay (Li and Wilkinson, 1998), and homozygous mice would be negative for Robo1 message and, hence, protein. In situ hybridization studies on wild-type and homozygous mutant E12.5 embryos revealed that Robo1 mRNA expression was completely absent in the Robo1 knockout, whereas Robo2 and Rig1 expression remained high in the spinal cord (Fig. 1F). Similarly, western blot analysis on whole embryo (E14.5) extracts, which were probed with an antiserum against the C terminus of Robo1 (205) (Xian et al., 2001), showed that Robo1 expression was high in the wild-type specimen, reduced in the heterozygote and completely absent in the knockout (Fig. 1G). As a control, western blots were stripped and re-probed with a β-actin antibody to demonstrate equal loading. These results indicate that our *Robo1* knockout mice produce no Robo1 mRNA or protein and thus should be considered as complete null mutants.

All phenotypic analyses described here were performed on *Robo1* mutant mice backcrossed onto the C57Bl/6 background for 6 to 10 generations. Complete mortality of homozygous deficient mice was seen at birth in the C57Bl/6 line.

Robo1, but not Robo2 is expressed on corpus callosum axons

We have previously shown, using an antibody directed against both Robo1 and Robo2, that Robo receptors are expressed on callosal axons (Shu et al., 2003a). However, the generation of antibodies by F. Murakami that recognize Robo1 and Robo2 independently (Long et al., 2004; Sabatier et al., 2004) has demonstrated that Robo1 is expressed at high levels on callosal axons at E17 (Fig. 2A,C,E), whereas Robo2 is only faintly expressed in this region (Fig. 2B,D). In the same brain, Robo2 is expressed at high levels on other axonal tracts within the brain such as the nigrostriatal pathway, the optic tract and, to a lesser extent, on axons within the internal capsule (Fig. 2F).

Robo1 knockout mice display unique malformations of the corpus callosum

Robo1 knockout brains from E17 and E18 embryos were first examined by DTMRI to identify large fibre tracts. This revealed gross abnormalities in the development of the corpus callosum and hippocampal commissure (Fig. 3 – shown at E17). DTMRI colour

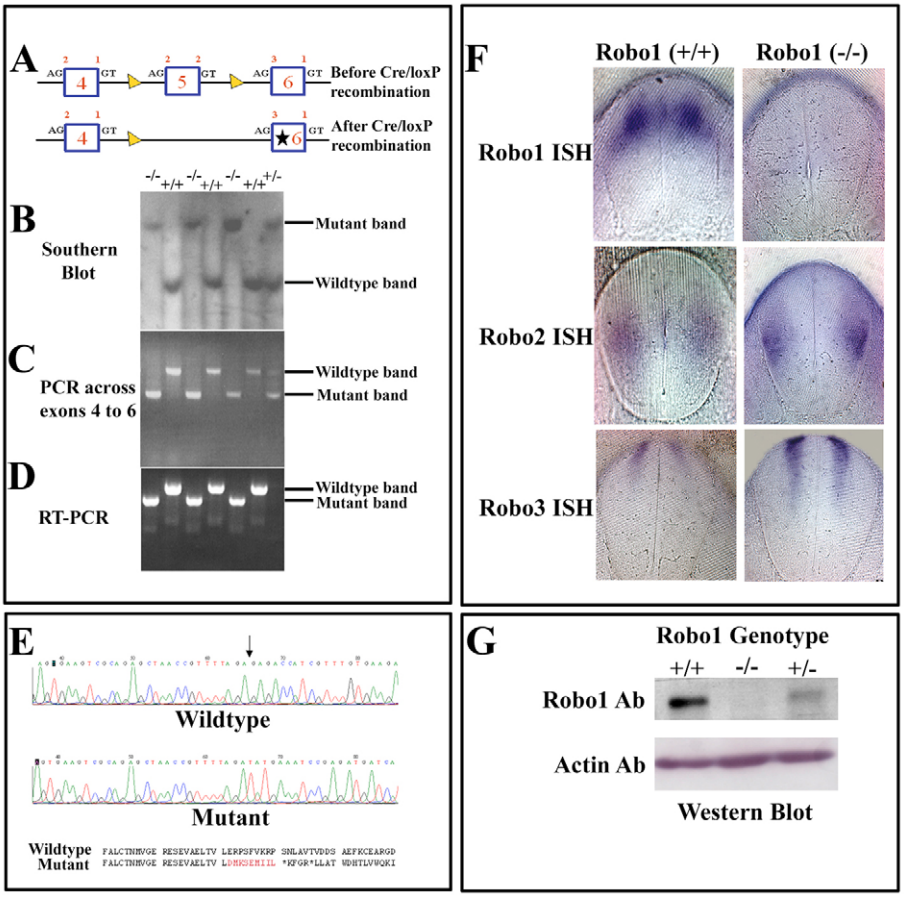

Fig. 1. Generation of conditional Robo1 knockout mice. (**A**) Exon structure (depicted by a square box) corresponding to Ig domains 2b, 3a and 3b (exons 4 to 6, respectively, indicated in red). The position of the terminal nucleotides within an amino acid codon is indicated above the exon in red. The yellow triangles shown in the upper panel represent lox P sites cloned into unique *Xba*I and *Kpn*I sites (loxP sites flanking a neo cassette, not shown in diagram). (**B**,**C**) Genotype analysis of tail DNA obtained from one F2 litter. Allele sizes are discriminated by the *Xba*I site that was 'silenced' by the cloning of the loxP site between exons 4 and 5 and probed with a genomic probe including exon 4 (B) or by PCR across exons 4 and 6 (C). (**D**) RT-PCR across exons 3 and 7 on mRNA isolated from wild-type and homozygous brains also confirmed that the deletion had occurred in the mutants. (**E**) The mRNA sequence of the RT-PCR products that were cloned into a TA vector. The lower panel (mutant) indicates the presence of multiple premature stop sites within the protein. (**F**) In situ hybridization was performed using probes against Robo1, Robo2 and Robo3. Robo1 mRNA was absent, but Robo2 and Robo3 mRNA were still expressed in the mutant. (**G**) Similarly, Robo1 protein was not expressed in the mutant as indicated by western blot analysis.

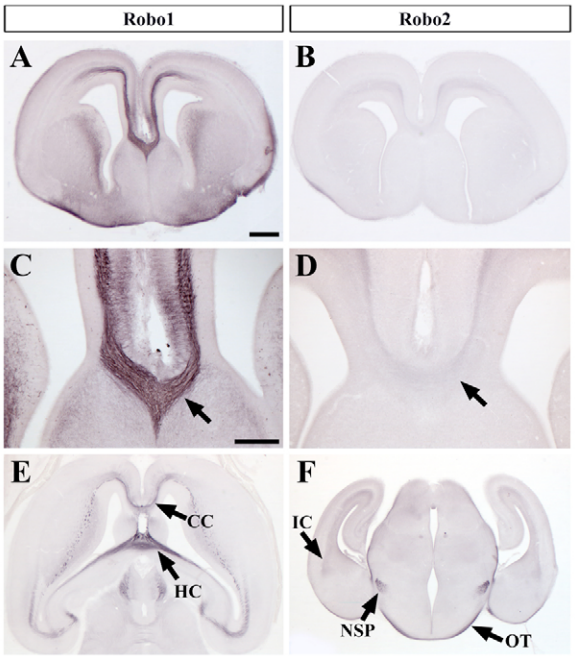

Fig. 2. Robo1 and Robo2 expression in the forebrain. Robo1 and Robo2 expression was examined using antibodies specific for each receptor. (**A-D**) In rostral sections, Robo1 protein was highly expressed on callosal axons at E17 (A, coronal view; arrow in C; C is a higher power view of A), whereas Robo2 staining is very faint (B, coronal view at E17; arrow in D; D is a higher power view of B). (**E**,**F**) In more caudal regions, Robo1 is expressed on the hippocampal commissure (HC) and on the corpus callosum (CC) (E, horizontal view at E17); Robo2 is expressed on the nigrostriatal pathway (NSP), the internal capsule (IC) and the optic tract (OT) (F, coronal view at E17). Scale bar in A: 200 μm for A,B,E,F; in C, 100 μm for C,D.

maps demonstrate the diffusion anisotropy of water molecules in ordered structures (Zhang et al., 2003) and can be 'colour-coded' to demonstrate axonal fibre tracts running in different orientations within the brain. In the horizontal plane, the presence of the corpus callosum (Fig. 3A, arrow in A′) and hippocampal commissure (Fig. 3A, arrowhead in A′) are shown in wild-type (n=3) and heterozygote (n=3) littermates. However, disruption in both of these tracts was evident in the knockout (n=2; Fig. 3G-I). A large reduction in the size of the corpus callosum and hippocampal commissure was observed in the mid-sagittal plane (compare green structures with a large arrow in Fig. 3C′ with Fig. 3I′). However, the anterior commissure was present in mice of each genotype (small arrow in Fig. 3C′,F′,I′). Coronal sections revealed that callosal axons in *Robo1* knockout mice were blue at the midline (Fig. 3H, arrow in H′) rather than green (Fig. 3B, arrow in B′), indicating that axons were coursing in the dorsoventral plane rather than mediolaterally. This could indicate that when callosal axons reach the midline, they turn to grow ventrally rather crossing the midline.

To further analyse the phenotype, sections (control mice, n=5; knockouts, n=2) were stained with an antibody against L1-CAM that labels all axons of the corpus callosum and projections from the hippocampus including the fimbria, fornix and hippocampal commissure (Fig. 4). Callosal axons and fibres in the fornix formed large fasciculated bundles at the midline in the knockout (Fig. 4I-L, arrows). Although some axons still crossed the midline (Fig. 4L,L′, asterisks), others were clearly mis-routed into these large fascicles. Mis-projection of callosal axons in the Robo1 knockout brain occurred throughout the tract at both rostral (Fig. 4K,K′) and caudal (Fig. 4L,L′) levels. Thus, rather than forming classic Probst bundles, callosal axons and axons of the hippocampal commissure formed tight fascicles that projected ventrally. This suggests that loss of Robo1 results in the formation of segregated axonal fascicles rather than the normal single bundle of axons that make up the corpus callosum. Our immunohistochemical analysis could not discern whether these fascicles were derived primarily from the cortex or the hippocampus as L1-CAM labels both projections. To examine these projections independently, we injected DiI into the cortex (n=6 knockouts) to label the callosal axons and DiA into the hippocampus (n=2 knockouts) to label the fornix and hippocampal commissure (Fig. 5). We found that in both the callosal and hippocampal commissure projections, the axons bundled together in large clusters that ectopically projected into the septum (rather than forming a single large bundle that crossed the midline; Fig. 5). The axons of the corpus callosum and hippocampal commissure normally remain segregated at all rostrocaudal levels (n=7 controls; overlays in Fig. 5E,J,O) and do not mix together. However, in Robo1 knockout brains, these large clusters of axons from the callosal and hippocampal projections were mixed (red and green bundles in the overlay Fig. 5I,N). An alternative phenotype would have been for single axons to mix between the two projections, but this was not observed. Thus, Robo1 appears to be involved in maintaining the complete segregation of these two commissures. Finally, as seen by immunohistochemical analysis above, some axons still crossed the midline in the rostral region (Fig. 5B, arrow).

Development of midline glial structures in *Robo1* knockout mice

Previous work has described midline glial structures that guide callosal axons at the midline (Silver, 1993; Shu and Richards, 2001). In order to examine these structures, we labelled brain sections with glial fibrillary acidic protein. All three midline glial populations were present – the glial wedge, indusium griseum glia and the midline zipper glia (Shu et al., 2003b) – in both wild-type (n=5; Fig. 6A,B) and *Robo1* knockout brains (n=2; Fig. 6C,D). Although some disruption of the midline zipper glia was evident (compare Fig. 6B,D), it appeared that this was secondary to the formation of the large axonal fascicles described above.

Advanced thalamocortical and corticothalamic projections in *Robo1* knockout mice

In Slit2 knockout mice, corticothalamic and thalamocortical projections deviate within the internal capsule resulting in an ectopic commissure (Bagri et al., 2002). To investigate these projections in Robo1 knockout mice, DiI and DiA crystals were placed in the dorsal thalamus and cortex, respectively, of wild-type and knockout littermate brains (E12.5-18.5; Fig. 7). At E12.5, similar to what has been described in the rat (Molnár and Cordery, 1999), we observed thalamocortical and corticothalamic fibres, bearing growth cones at their tips, growing out of their sites of origin and directed towards the region of the internal capsule. There was no apparent difference in the pattern or extent of labelling between mutant and Robo1 wild-type mice (n=3 for each condition, data not shown). However, at E14.5, although both thalamocortical and corticothalamic projections in knockout brains (n=4) followed paths comparable with those in wild type (n=4), they were further advanced. Thus, although axons of both systems in wild-type brains had not advanced past the lateral cortex (Fig. 7D,E), thalamocortical projections (DiI,

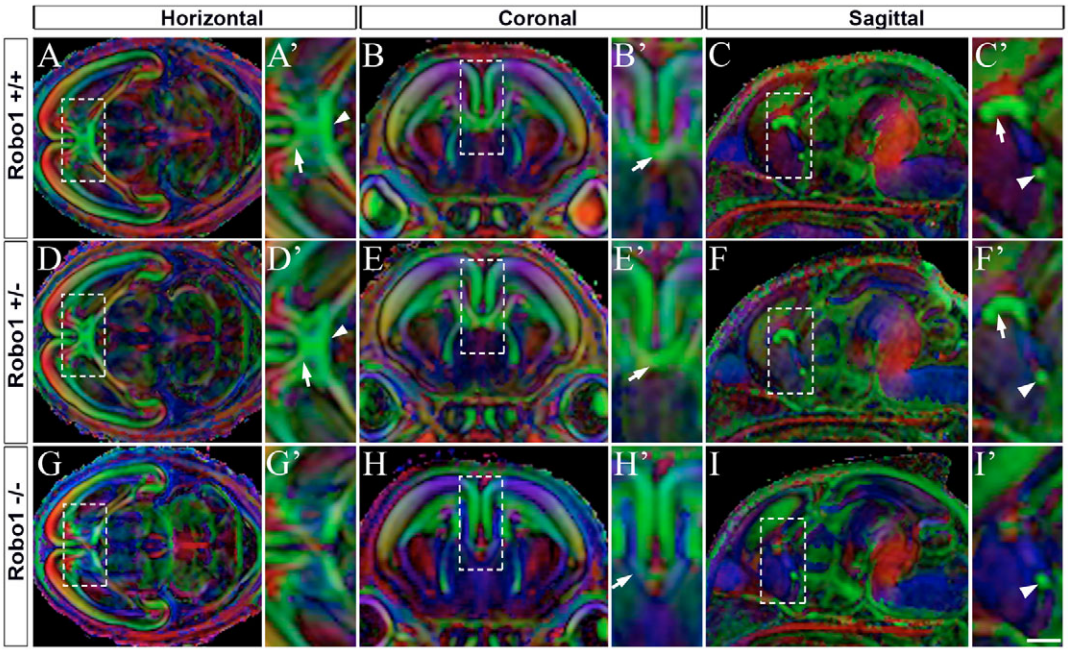

Fig. 3. Magnetic resonance diffusion tensor imaging of Robo1 knockout brains. To survey the entire brain for axonal tract defects, we scanned Robo1 and control littermate brains in a 9.4 Tesla magnet. In these images, orientations of axonal tracts are pseudo-coloured according to their orientation within the brain. Axonal tracts projecting mediolaterally, such as commissures, are green; tracts projecting in the dorsoventral axis are blue; and tracts in the rostrocaudal axis are red. Brains from wild-type (**A-C**), heterozygote (**D-F**) and *Robo1* knockout (**G-I**) littermates were analyzed at E17. (A′-I′) Higher power views of the boxed regions in A-I, respectively. Three planes of section were extracted from the 3D data and are shown at the level of the rostral corpus callosum: horizontal (A,D,G); coronal (B,E,H) and sagittal (C,F,I). The corpus callosum is indicated by the arrows in the wild-type brain in A′-C′ and in the knockout in G′-I′. The anterior commissure is observed as a green spot in cross-section and indicated by the arrowheads in C′,F′,I′. From this analysis, it is evident that the corpus callosum (arrow in A′) and hippocampal commissure (arrowhead in A′) are greatly reduced in the *Robo1* knockout (compare A′ with G′, and C′ with I′) and that the orientation of the fibres has changed from mediolaterally (green) to dorsoventrally (blue) projecting. Scale bar: 650 μm for A,D,G; 400 μm for B,E,F; 500 μm for C,F,I; 250 μm for B′,C′,E′,F′,H′,I′; 350 μm for A′,D′,G′.

red) in the knockouts were observed well into the cortex (compare Fig. 7A with 7D) where a few cortical plate cells had been back-labelled (Fig. 7B, arrows). Similarly, the corticothalamic projections in these animals (DiA, green) were already present in the thalamus (Fig. 7A). Furthermore, DiI-labelled axons crossing transversely over the thalamocortical fibre bundle were observed at the level of the internal capsule. This ‘knot’ structure (Fig. 7C, arrow), observed in all knockout brains examined at this age, could be the result of a misplaced subgroup of thalamic axons or other misrouted axons such as retrogradely labelled optic tract axons. These data indicate that early in development, Robo1 plays a role in the timely projection of thalamocortical and corticofugal axons. Examination of E18.5 brains (n=4 for each condition) showed the advance of thalamocortical axons persisted in the *Robo1* knockouts where the axons projected further medially into the cortex (Fig. 7G, arrow) compared with controls (Fig. 7K, arrow). In addition, back-labelled cells appeared in greater numbers in the thalamus of mutants following placement of dye in the cortex (compare Fig. 7I with 7M, arrows), further indicating that thalamocortical axons had arrived earlier in these brains. Furthermore, similar to DTMRI analysis, we observed corpus callosum axons deviating ventrally at the midline (Fig. 7F, arrow). In addition, similar to E14.5, DiI-labelled axons coursing transversely at the level of the internal capsule formed a ‘knot’ structure in all but one of the Robo1 knockout brains examined (Fig. 7H, arrow), while they were absent in the controls (Fig. 7L, arrow).

The distribution of interneurons in the cerebral cortex of Robo1 knockout mice

Robo1 mRNA is localized in the developing neocortex and the proliferative zone of the GE (Marillat et al., 2002), suggesting that this receptor may regulate the movement of cortical interneurons from the ventral telencephalon. We examined Robo1 expression in coronal sections of E13.5 and E15.5 mouse brains, ages when interneuron migration is at its peak. Staining was identified in the mantle zone of the GE and along the marginal zone (MZ) and lower intermediate zone (IZ) of the cortex (Fig. 8A), well-defined routes for tangentially migrating interneurons (Fig. 8B) (Anderson et al., 1997; Parnavelas, 2000). The staining in these zones was rather dense and it was difficult to discern individual cell bodies from processes oriented parallel to the ventricular surface. At high magnification, the Robo1 receptor was clearly visualized in some individual cells, especially in the GE near the start of the migratory route (Fig. 8A′). These cells often displayed elongated somata and leading processes, features typical of migrating interneurons. Further analysis of dissociated GE cell cultures prepared from E15 animals showed Robo1 expression in GABAergic cells as identified by co-labelling with GAD65 (Fig. 8C-E).

A number of studies have reported that interneurons use corticofugal projections to migrate from the ventral telencephalon to the cortex (Parnavelas, 2000; Denaxa et al., 2001; Morante-Oria et al., 2003; McManus et al., 2004), although such an association has not been supported by the work of others (Tanaka

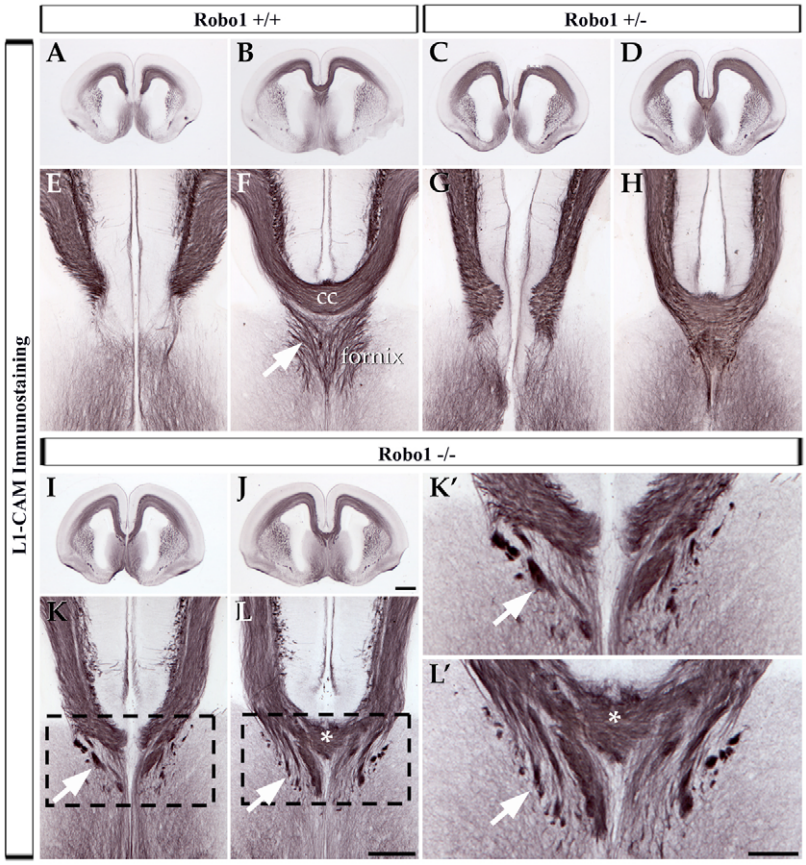

Fig. 4. *Robo1* knockout mice display aberrant axonal pathfinding in the corpus callosum and hippocampal commissure. (**A-H**) Coronal brain sections taken at the rostral level of littermates of *Robo1* mice were labelled with L1-CAM immunohistochemistry to reveal axonal projections in the corpus callosum (CC) and fornix/hippocampal commissure at E17.5. In wild-type (A,B,E,F) and heterozygous (C,D,G,H) mice, both callosal and hippocampal projections appeared normal. However, in knockout littermates, medially projecting axons formed tight fascicles that failed to cross the midline (white arrows in K,K′,L,L′). Sections of the same brain from rostral (**I**,**K**) to caudal (**J**,**L**) indicated that axons along the rostrocaudal extent of these commissures were disrupted (I-L). Some axons still crossed the midline (asterisks in L,L′), indicating that not all callosal axons were affected. E-H and K,L are higher power images of A-D and I,J, respectively. K′ and L′ are higher power views of the boxed regions in K and L, respectively. Scale bars: in J, 200 μm for A-D,I,J; in L, 100 μm for E-H,K,L and 50 μm for K′,L′.

et al., 2003). Thus, given the defects observed in the corticofugal projections, we wanted to elucidate the possible role of Robo1 in interneuron migration and distribution in the cortex. We examined brain sections (E12.5-E18.5) stained for calbindin, a marker of cortical interneurons. Although not all interneurons express calbindin (López-Bendito et al., 2004), this marker has been used routinely to label a large subpopulation of GABAergic interneurons migrating tangentially to the cortex (Anderson et al., 1997; Sussel et al., 1999). Our results clearly showed that the pattern of calbindin staining closely resembled that of Robo1 immunoreactivity (Fig. 8A,B). Analysis of wild-type E12.5 mice showed relatively few calbindin-positive cells predominantly in the lateral cortex (Fig. 9D) in agreement with earlier observations (Anderson et al., 1999; Anderson et al., 2001). However, in Robo1 knockout littermates, significantly more calbindin-positive cells were observed in the cortex (Fig. 9E). Cell counts at E12.5 (n=4 for each condition) revealed that almost twice as many calbindin-positive neurons had migrated into the cortices of *Robo1*

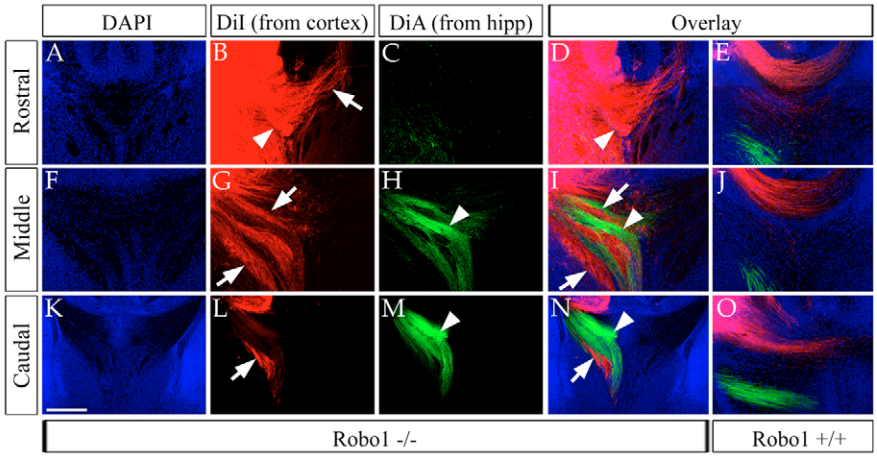

Fig. 5. Tract tracing analysis reveals major pathfinding defects in callosal and hippocampal axons. (**A-O**) Dual tract tracing was performed at E17.5 by labelling the callosal projection with DiI in the medial cortex (red label in the figure) and labelling the hippocampal projection through the fornix and hippocampal commissure with DiA in the dentate gyrus (green label in the figure). Coronal sections were counterstained with DAPI (A,F,K). Brains were analysed from rostral to caudal at the level of the corpus callosum and hippocampal commissure. (There is no green labelling in C as this section is rostral to the fornix and HC.) In *Robo1* knockout mice, callosal (B, arrowhead; G and L, arrows) and hippocampal (arrowheads in H and M) axons formed tight fascicles that did not cross the midline. Furthermore, fascicles from both the cortex and hippocampal projections overlapped at the midline (knockout overlay images are in I and N), whereas in wild-type mice these projections remained completely separate (E,J,O). As observed by immunohistochemical analysis, tract tracing analysis revealed axons crossing the midline in the rostral region of this *Robo1* knockout brain (arrow in B; D, overlay). Scale bar: 200 μm.

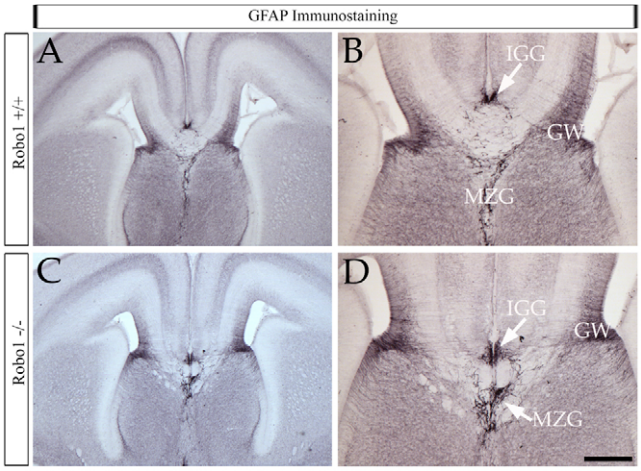

Fig. 6. Midline glial populations are present in Robo1 knockout mice. (**A-D**) To assess the development of midline glial structures in Robo1 knockout (C,D) or control (A,B) mice, E17.5 brains were sectioned coronally and labelled by glial fibrillary acidic protein (GFAP) immunohistochemistry. Three midline glial populations were present: the glial wedge (GW), glia within the indusium griseum (arrow labelled IGG in B and D) and the midline zipper glia (MZG) in both wild-type and *Robo1* knockout brains. Some abnormalities were noted in the MZG but this is probably due to the morphological disruption within the area by the formation of large axon fascicles and the lack of a definitive corpus callosum (arrow labelled MZG in D). Scale bar: 400 μm in A,C; 200 μm in B,D.

knockouts (220±12, $P<0.001$) compared with controls (98±10) (Fig. 9A,D,E). A comparable increase in the number of calbindin-positive cells was noted in the cortex of *Robo1* knockouts at E15.5 ($n=4$ for each condition).

Analysis at E18.5 ($n=3$ for each condition) demonstrated an ~35% increase in the total number of calbindin-positive cells counted in a 200 μm wide strip of knockout dorsomedial cortex (DMC) compared with counts in a similar area in wild-type brains (Fig. 9B). Counts at different levels along the rostrocaudal axis showed that the increased number of calbindin-positive cells was evident in rostral (Fig. 9C,D,E) and middle (parietal) cortical areas (Fig. 9C,F,G), but not in the caudal (occipital) cortex (Fig. 9C). Furthermore, there was an abundance of calbindin-positive cells in the striatal region (Fig. 9G,G′, arrows), an area that is normally repulsive to migrating interneurons (Marín et al., 2001). The presence of calbindin labelled cells in the striatum was also evident in E15.5 knockout brains (data not shown). These observations indicate that Robo1 influences both the number of interneurons entering the cortex early and their migratory route through the ventral telencephalon.

DISCUSSION

Evidence presented here and elsewhere suggests that although the cellular processes involved in cell migration and axon guidance are fundamentally different, similar molecules may be involved. Here, we have found that Robo1 is indeed involved in both cell migration, and axon growth and guidance events. Furthermore, we found significant differences between the phenotype of Robo1 knockout mice and that of *Slit2* or *Slit1/2* double knockout mice. The largest differences are

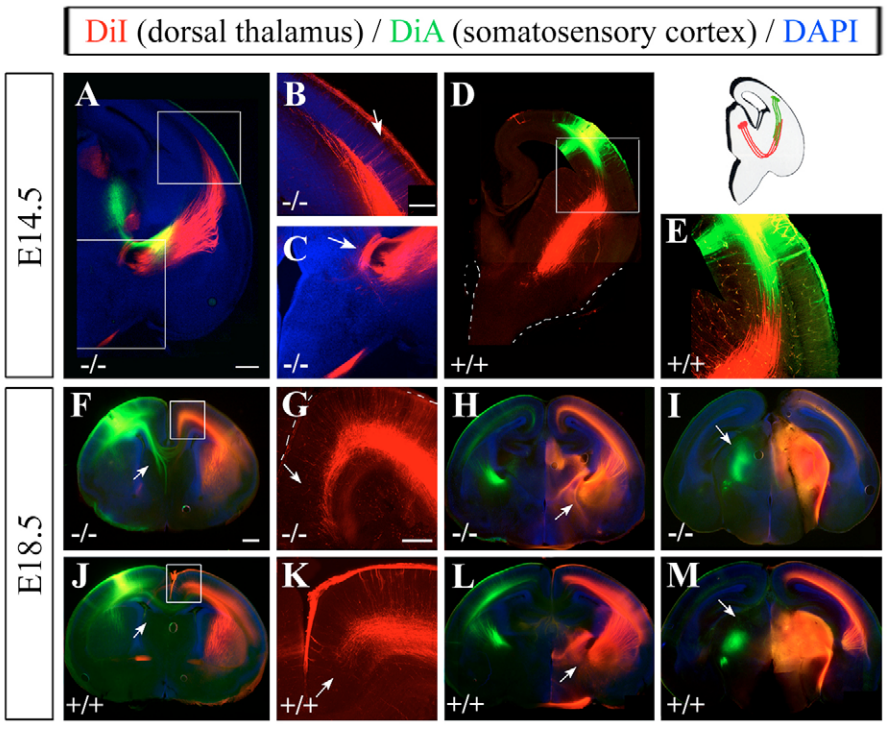

Fig. 7. Thalamocortical and corticofugal axons advance faster towards their respective targets in Robo1 knockout brains. DiI was placed in the dorsal thalamus to label thalamocortical axons (red in all panels and in schematic diagram) and DiA was placed in the presumptive somatosensory cortex of the same brains to label corticofugal axons (green in all panels and in schematic diagram) at either E14.5 (**A-E**) or E18.5 (**F-M**). *Robo1* knockout brains (A-C,F-I) were compared with controls (D,E,J-M) in coronal sections of middle and caudal regions. At E14.5, thalamocortical axons in the knockout (A,B; arrow in B indicates retrograde labelling of cortical cells) advanced further into the cortex than in wild-type littermates (D,E) which had not yet passed the corticostriatal notch. Similarly, corticofugal axons had already reached the thalamus in E14.5 *Robo1* knockout brains (A), but had not yet entered the striatum in controls (D,E). (B,C) Higher power views of the boxed regions in A (red and blue channels only). At E14.5 and E18.5, we observed an aberrant projection of DiI-labelled axons coursing transversely over the axons of the internal capsule in *Robo1* knockout brains in a 'knot'-like structure (arrows in C and H), but not in controls (D and arrow in L). As observed in Fig. 5, most callosal axons (labelled here with DiA) projected aberrantly into the septum of *Robo1* knockouts (F, arrow) compared with controls (J, arrow). (G,K) Higher power views of the boxed regions in F,J (red channel only). The advance of thalamocortical axons persisted at E18.5 in the *Robo1* knockout, where these axons projected further medially into the cortex (G, arrow) compared with controls (K, arrow). Furthermore, back-labelled cells appeared in greater numbers in the thalamus of mutants following placement of dye in the cortex (compare I with M, arrow), further confirming that thalamocortical axons had arrived earlier in these brains. Scale bars: in A, 400 μm in A,D; in B, 200 μm in B,C; in F, 400 μm in F,H,I,J,L,M; in G, 200 μm in G,K.

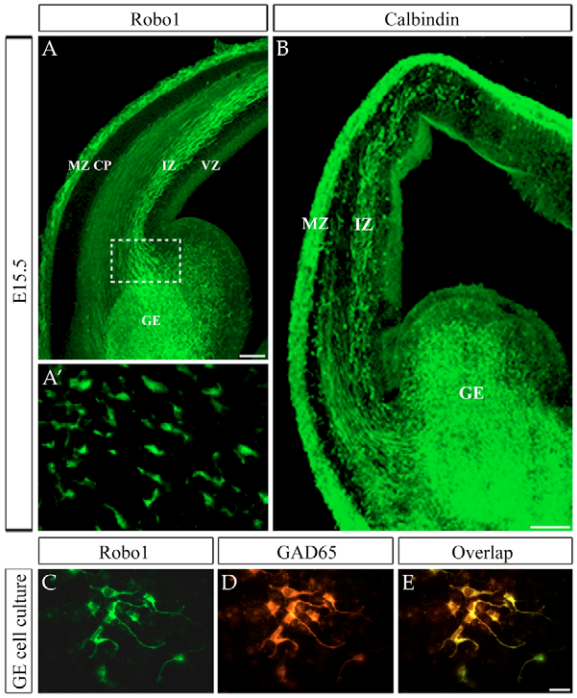

Fig. 8. Robo1, calbindin and GAD65 immunohistochemistry of cells from the ganglionic eminence. (**A**) Image of a wild-type coronal section showing robust Robo1 staining in the mantle zone of the ganglionic eminence (GE) and in two bands in the marginal zone (MZ) and lower intermediate zone (IZ) of the developing cortex. At high magnification, the receptor was clearly localized in some individual cells, especially near the corticostriatal notch, that showed features of migrating neurons (boxed area is shown at higher magnification in A′). (**B**) Similar to Robo1 staining, calbindin immunoreactivity was localized chiefly in the GE, and in the corridors within the cortex used by migrating cortical interneurons, the MZ and lower IZ. (**C-E**) Dissociated GE cell cultures prepared from an E15 wild-type animals were co-stained with Robo1 (C) and GAD65 (D), showing that GABAergic cells in this part of the ventral telencephalon express the receptor (E, a composite of C and D). Scale bars: 200 μm in A,B; in E, 10 μm in A′ and 35 μm in C-E.

in the formation of the corticothalamic and thalamocortical pathfinding between the two types of mutants and in the migration of interneurons to the neocortex from the ventral forebrain. *Slit2* or *Slit1/2* double mutants display large ectopic commissures in the diencephalon that are made up of axons from the cortex which would normally project to the thalamus (Bagri et al., 2002). Thalamocortical axons in these mice display ectopic projections ventrally and very few enter the cortical plate. However, in Robo1 knockouts, thalamocortical and corticothalamic axons reach their targets at least one day earlier than in controls and no ectopic commissures are present in the diencephalon. Furthermore, previous data show no defect in interneuron migration into the cortex of Slit or Slit/Netrin (Ntn) mutants (Marín et al., 2003), whereas we see an increase, compared with controls, in the number of interneurons entering the cortex and reaching their targets early. These differences are significant and imply one of three possibilities for Slit signalling in this system: (1) both Robo1 and Robo2 are required for Slit signalling; (2) Robo1, together with an unknown receptor is required for Slit signalling, or (3) a completely novel Slit receptor is involved in these processes. An additional possibility is that Robo1 acts alone (possibly as a homodimer) in one of more of these systems.

Robo1 is required for the formation of the corpus callosum and hippocampal commissure

The role of Slit2 in callosal formation has been demonstrated in vivo using both gene mutation and antisense knockdown of the protein (Bagri et al., 2002; Shu et al., 2003a). However, the Robo receptor involved has been unclear. Our data show that Robo1 is required for callosal formation, but some subtle differences also exist between the Robo1 and Slit2 callosal phenotypes. For example, when Slit2 is removed, axons tend to defasciculate (Bagri et al., 2002; Plump et al., 2002; Shu et al., 2003a), whereas when Robo1 is absent, the axons form tight axon clusters or bundles that project ectopically en masse (data presented here). Our data also suggest that Robo1 might be involved in maintaining a crucial distance between callosal and hippocampal commissure axons. Our finding that axon bundles from each commissure were mixed together at the midline, rather than remaining segregated, suggests the involvement of Robo1 in normally maintaining the separation of these commissures into two distinct fibre tracts, perhaps either through Robo/Slit signalling or through Robo1 homophilic interactions.

Robo1 regulates the timing of corticothalamic and thalamocortical targeting

Our results demonstrate that corticothalamic and thalamocortical projections reach their targets prematurely when compared with their wild-type littermates early in development. This may be interpreted in one of two ways: either Robo1 normally acts as a growth retardant for these axons in a Slit-independent manner; or the interactions between Robo1 and either Slit1 expressed in the cortical plate (Whitford et al., 2002) or Slit1 and Slit2 expressed in the thalamus (Marillat et al., 2002; Bagri et al., 2002), prevent these axons from entering their respective targets until later. *Slit2* and *Slit1/2* double mutants display major pathfinding defects in the formation of these projections (Bagri et al., 2002). However, the pathfinding defects were not observed in the Robo1 knockouts (other than overshooting their targets at each age as described). Hence, either these effects are mediated by a different receptor or by a different combination of receptors. The finding that Robo2 is not highly expressed on callosal axons makes it unlikely that elimination of both Robo1 and Robo2 simultaneously might be required to observe similar defects as those described in Slit mutants. Regardless, we and others (Long et al., 2004) have been unable to generate *Robo1* and *Robo2* double knockout mice by breeding owing to the proximity of these two genes on the same chromosome. We found that Robo1 is expressed in axons within the IZ at a time when both the corticofugal and thalamocortical axonal systems develop. By E18.5, when these axons have reached their final targets, Robo1 labelling is downregulated in these axons. Thus, the phenotype observed in the mutants might be directly mediated by Robo1 on the developing axons in the cortex. In addition, Robo1 is expressed within the GE and could, therefore, mediate guidance events on both thalamic and cortical projections within this region.

Robo1 affects the migration of cortical interneurons from the ventral telencephalon

Our results show a significant increase in the number of interneurons that enter the cerebral cortex from the ventral forebrain in *Robo1*-null mice throughout the period of corticogenesis. Furthermore, we found that these neurons migrated through the striatum and were not repelled by it. Previous studies have shown that the striatum expresses Sema3a and Sema3f (Marín et al., 2001), and GABAergic interneurons expressing neruopilin 1 (Npn1) are repelled away from the striatum into the cortex (Marín et al., 2001; Morante-Oria et al.,

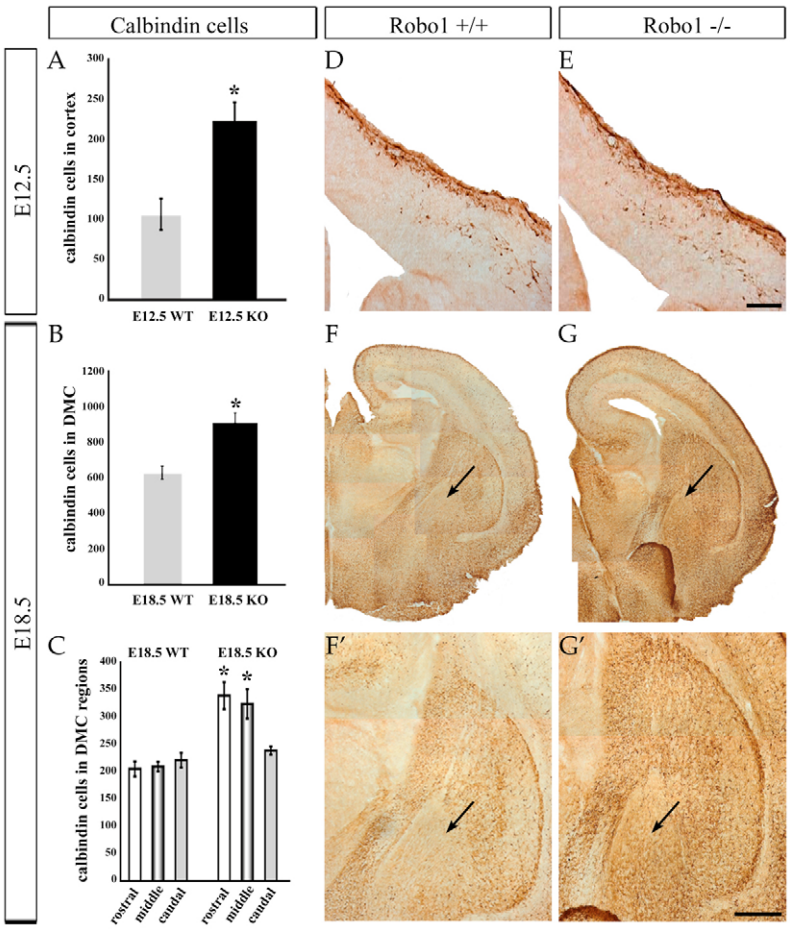

Fig. 9. Cell migration defects in the forebrain of Robo1 knockout brains. (**A**) Quantification of the total number of calbindin labelled cells that entered the cortex of control and *Robo1* knockout brains at E12.5 showed that the latter contained roughly twice as many cells (*P<0.001, Student's t-test; error bars represent s.e.m.). (**B**) Histogram depicts the average number of calbindin cells in a 200 μm wide radial strip of dorsomedial cortex (DMC) in control and *Robo1* knockout brain sections at E18.5. More calbindin-positive cells were observed in the knockout cortex (*P<0.01, Student's t-test; error bars represent s.e.m.). (**C**) At E18.5, the average number of calbindin cells in rostral and middle regions (200 μm wide strip) of DMC is higher in *Robo1* knockout brains compared with control (*P<0.01 for both rostral and middle regions, Student's t-test; error bars represent s.e.m.), whereas no difference was observed in caudal regions. Calbindin staining in representative coronal sections taken from rostral cortex at E12.5 (**D**,**E**) and middle (parietal) cortex at E18.5 (**F-G**′) of control (D,F) and Robo1 knockout (E,G) mouse brains. The cortex of the knockout brains appeared to contain a greater number of calbindin-labelled cells. The arrows in F,G indicate the striatal region, shown at higher magnification at F′ and G′, which is populated by calbindin cells in Robo1 knockout brains (G,G′), but not in controls (F,F′). Scale bars: in E, 200 μm in D,E; in G′, 400 μm in F,G and 200 μm in F′,G′.

2003). Slits have also been shown to repel GABAergic interneurons in vitro (Zhu et al., 1999). However, in vivo, *Slit1/2* double knockout mice and *Slit1/2* and *Ntn1* triple knockout mice do not display defects in cortical interneuron migration (Marín et al., 2003). It is difficult to reconcile these data with our findings and explain why in the Robo1 knockout animals, interneurons migrate through the repulsive striatal region and enter the cortex earlier and in larger numbers than normal.

The data suggest that there may be two different developmental events occurring. First, that Robo1 is required to repel the cells around the striatum, which may be a Slit-dependent or independent event. Neurons still avoid the striatal area in *Slit1/2* double mutant mice (Marín et al., 2003), indicating that this might be a Slit-independent event. However, presumably these neurons still express Npn1 and the striatal region would still express Sema3a and Sema3f. Thus, perhaps, both Npn1/Sema and Robo1 signalling are required to steer the cells around the striatum. The second abnormal developmental event we observed is that more interneurons migrate into the cortex. The most plausible explanation for this is that these cells follow the cortical and thalamic axons within the internal capsule that enter their respective targets earlier than normal in *Robo1* knockout mice. A close association with the TAG-1 expressing axonal bundles of the developing corticofugal fibre system has been observed, prompting speculation that interneurons use this system as a scaffold for their migration into the neocortex (Denaxa et al., 2001; Morante-Oria et al., 2003; McManus et al., 2004). Considering that Robo1 is expressed in the GE, where interneurons originate from, and in the IZ, a zone that contains the majority of migrating interneurons to the cortex, it is possible that their trajectory is both directly delineated by Robo1 and indirectly regulated through fasciculation and migration along cortical and thalamic axons.

Why was the increase in interneuron number restricted to the rostral and middle cortical areas of the *Robo1* knockout mice? Recent studies by Yozu et al. (Yozu et al., 2005) have clearly shown that the sources and mechanisms of migration of interneurons that populate these areas are different from those destined for caudal cortical regions. Specifically, these investigators have demonstrated that interneurons destined for the caudal cortex and hippocampus arise in the caudal GE and use a novel migratory path, the so-called caudal migratory stream, whereas those that populate rostral and middle areas arise predominantly from the MGE/LGE. Finally, we cannot exclude the possibility that the increase in interneuron numbers in the rostral and middle cortical areas is due to a differential increase in proliferation in different parts of the GE.

In summary, we found that Robo1 is required for the correct formation of the corpus callosum and the hippocampal commissure, as well as the timely projection of thalamocortical and corticofugal axons. In addition, the absence of Robo1 led to premature migration of interneurons to the cortex. The differences between the Robo1 knockout phenotype and the phenotypes of Slit-deficient mice suggest that additional components contribute to Robo/Slit signal transduction mechanism.

The authors gratefully acknowledge the contribution of Melissa Barber for Robo1 labelling. V.S. was a recipient of an MRC (UK) Career Establishment Award. The work in J.P.'s laboratory was supported by a Wellcome Trust Grant (074549). Work in L.J.R.'s laboratory was supported by a grant (FY05-785) from The March of Dimes Foundation for Birth Defects. Work in S.M.'s laboratory was supported by NIH grant EB003543-01A.

References

Anderson, S. A., Eisenstat, D. D., Shi, L. and Rubenstein, J. L. (1997). Interneuron migration from basal forebrain to neocortex: dependence on Dlx genes. *Science* **278**, 474-476.

Anderson, S., Mione, M., Yun, K. and Rubenstein, J. L. (1999). Differential origins of neocortical projection and local circuit neurons: role of Dlx genes in neocortical interneuronogenesis. *Cereb. Cortex* **9**, 646-654.

Anderson, S. A., Marín, O., Horn, C., Jennings, K. and Rubenstein, J. L. (2001). Distinct cortical migrations from the medial and lateral ganglionic eminences. *Development* **128**, 353-363.

Bagri, A., Marín, O., Plump, A. S., Mak, J., Pleasure, S. J., Rubenstein, J. L. and Tessier-Lavigne, M. (2002). Slit proteins prevent midline crossing and determine the dorsoventral position of major axonal pathways in the mammalian forebrain. *Neuron* **33**, 233-248.

Brose, K., Bland, K. S., Wang, K. H., Arnott, D., Henzel, W., Goodman, C. S., Tessier-Lavigne, M. and Kidd, T. (1999). Slit proteins bind Robo receptors and have an evolutionarily conserved role in repulsive axon guidance. *Cell* **96**, 795-806.

Camurri, L., Mambetisaeva, E. and Sundaresan, V. (2004). Rig-1 a new member of Robo family genes exhibits distinct pattern of expression during mouse development. *Gene Expr. Patt.* **4**, 99-103.

Cavanagh, J. F., Mione, M. C., Pappas, I. S. and Parnavelas, J. G. (1997). Basic fibroblast growth factors prolongs the proliferation of rat cortical progenitor cells in vitro without altering their cell cycle parameters. *Cereb. Cortex* **4**, 293-302.

Denaxa, M., Chan, C. H., Schachner, M., Parnavelas, J. G. and Karagogeos, D. (2001). The adhesion molecule TAG-1 mediates the migration of cortical interneurons from the ganglionic eminence along the corticofugal fiber system. *Development* **128**, 4635-4644.

Henrique, D., Adam, J., Myat, A., Chitnis, A., Lewis, J. and Ish-Horowicz, D. (1995). Expression of a Delta homologue in prospective neurons in the chick. *Nature* **375**, 787-790.

Hivert, B., Liu, Z., Chuang, C. Y., Doherty, P. and Sundaresan, V. (2002). Robo1 and Robo2 are homophilic binding molecules that promote axonal growth. *Mol. Cell. Neurosci.* **21**, 534-545.

Hu, H. (1999). Chemorepulsion of neuronal migration by Slit2 in the developing mammalian forebrain. *Neuron* **23**, 703-711.

Kidd, T., Brose, K., Mitchell, K. J., Fetter, R. D., Tessier-Lavigne, M., Goodman, C. S. and Tear, G. (1998a). Roundabout controls axon crossing of the CNS midline and defines a novel subfamily of evolutionarily conserved guidance receptors. *Cell* **92**, 205-215.

Kidd, T., Russell, C., Goodman, C. S. and Tear, G. (1998b). Dosage-sensitive and complementary functions of roundabout and commissureless control axon crossing of the CNS midline. *Neuron* **20**, 25-33.

Li, S. and Wilkinson, M. F. (1998). Nonsense surveillance in lymphocytes? *Immunity* **8**, 135-141.

Long, H., Sabatier, C., Ma, L., Plump, A., Yuan, W., Ornitz, D. M., Tamada, A., Murakami, F., Goodman, C. S. and Tessier-Lavigne, M. (2004). Conserved roles for Slit and Robo proteins in midline commissural axon guidance. *Neuron* **42**, 213-223.

López-Bendito, G., Sturgess, K., Erdelyi, F., Szabo, G., Molnar, Z. and Paulsen, O. (2004). Preferential origin and layer destination of GAD65-GFP cortical interneurons. *Cereb. Cortex* **14**, 1122-1133.

Marillat, V., Cases, O., Nguyen-Ba-Charvet, K. T., Tessier-Lavigne, M., Sotelo, C. and Chedotal, A. (2002). Spatiotemporal expression patterns of slit and robo genes in the rat brain. *J. Comp. Neurol.* **442**, 130-155.

Marín, O., Yaron, A., Bagri, A., Tessier-Lavigne, M. and Rubenstein, J. L. (2001). Sorting of striatal and cortical interneurons regulated by semaphorin-neuropilin interactions. *Science* **293**, 872-875.

Marín, O., Plump, A. S., Flames, N., Sanchez-Camacho, C., Tessier-Lavigne, M. and Rubenstein, J. L. (2003). Directional guidance of interneuron migration to the cerebral cortex relies on subcortical Slit1/2-independent repulsion and cortical attraction. *Development* **130**, 1889-1901.

McManus, M. F., Nasrallah, I. M., Gopal, P. P., Baek, W. S. and Golden, J. A. (2004). Axon mediated interneuron migration. *J. Neuropathol. Exp. Neurol.* **63**, 932-941.

Métin, C. and Godement, P. (1996). The ganglionic eminence may be an intermediate target for corticofugal and thalamocortical axons. *J. Neurosci.* **16**, 3219-3235.

Molnár, Z. and Cordery, P. (1999). Connections between cells of the internal capsule, thalamus and cerebral cortex in embryonic rat. *J. Comp. Neurol.* **413**, 1-25.

Molnár, Z., Adams, R. and Blakemore, C. (1998). Mechanisms underlying the early establishment of thalamocortical connections in the rat. *J. Neurosci.* **18**, 5723-5745.

Morante-Oria, J., Carleton, A., Ortino, B., Kremer, E. J., Fairen, A. and Lledo, P. M. (2003). Subpallial origin of a population of projecting pioneer neurons during corticogenesis. *Proc. Natl. Acad. Sci. USA* **100**, 12468-12473.

Mori, S. and van Zijl, P. C. (1998). A motion correction scheme by twin-echo navigation for diffusion-weighted magnetic resonance imaging with multiple RF echo acquisition. *Magn. Reson. Med.* **40**, 511-516.

Ozdinler, P. H. and Erzurumlu, R. S. (2002). Slit2, a branching-arborization factor for sensory axons in the Mammalian CNS. *J. Neurosci.* **22**, 4540-4549.

Parnavelas, J. G. (2000). The origin and migration of cortical neurones: new vistas. *Trends Neurosci.* **23**, 126-131.

Plump, A. S., Erskine, L., Sabatier, C., Brose, K., Epstein, C. J., Goodman, C. S., Mason, C. A. and Tessier-Lavigne, M. (2002). Slit1 and Slit2 cooperate to prevent premature midline crossing of retinal axons in the mouse visual system. *Neuron* **33**, 219-232.

Sabatier, C., Plump, A. S., Le, M., Brose, K., Tamada, A., Murakami, F., Lee, E. Y. and Tessier-Lavigne, M. (2004). The divergent Robo family protein rig-1/Robo3 is a negative regulator of slit responsiveness required for midline crossing by commissural axons. *Cell* **117**, 157-169.

Sang, Q., Wu, J., Rao, Y., Hsueh, Y. P. and Tan, S. S. (2002). Slit promotes branching and elongation of neurites of interneurons but not projection neurons from the developing telencephalon. *Mol. Cell Neurosci.* **21**, 250-265.

Shu, T. and Richards, L. J. (2001). Cortical axon guidance by the glial wedge during the development of the corpus callosum. *J. Neurosci.* **21**, 2749-2758.

Shu, T., Valentino, K. M., Seaman, C., Cooper, H. M. and Richards, L. J. (2000). Expression of the netrin-1 receptor deleted in colorectal cancer (DCC) is largely confined to projecting neurons in the developing forebrain. *J. Comp. Neurol.* **416**, 201-212.

Shu, T., Sundaresan, V., McCarthy, M. M. and Richards, L. J. (2003a). Slit2 guides both precrossing and postcrossing callosal axons at the midline in vivo. *J. Neurosci.* **23**, 8176-8184.

Shu, T., Puche, A. C. and Richards, L. J. (2003b). Development of midline glial populations at the corticoseptal boundary. *J. Neurobiol.* **57**, 81-94.

Silver, J. (1993). Glia-neuron interactions at the midline of the developing mammalian brain and spinal cord. *Perspect. Dev. Neurobiol.* **1**, 227-236.

Sundaresan, V., Mambetisaeva, E., Andrews, W., Annan, A., Knoll, B., Tear, G. and Bannister, L. (2004). Dynamic expression patterns of Robo (Robo1 and Robo2) in the developing murine central nervous system. *J. Comp. Neurol.* **468**, 467-481.

Sussel, L., Marín, O., Kimura, S. and Rubenstein, J. L. (1999). Loss of Nkx2.1 homeobox gene function results in a ventral to dorsal molecular respecification within the basal telencephalon: evidence for a transformation of the pallidum into the striatum. *Development* **126**, 3359-3370.

Tanaka, D., Nakaya, Y., Yanagawa, Y., Obata, K. and Murakami, F. (2003). Multimodal tangential migration of neocortical GABAergic neurons independent of GPI-anchored proteins. *Development* **130**, 5803-5813.

Wang, K. H., Brose, K., Arnott, D., Kidd, T., Goodman, C. S., Henzel, W. and Tessier-Lavigne, M. (1999). Biochemical purification of a mammalian slit protein as a positive regulator of sensory axon elongation and branching. *Cell* **96**, 771-784.

Westin, C. F., Maier, S. E., Mamata, H., Nabavi, A., Jolesz, F. A. and Kikinis, R. (2002). Processing and visualization for diffusion tensor MRI. *Med. Image Anal.* **6**, 93-108.

Whitford, K. L., Marillat, V., Stein, E., Goodman, C. S., Tessier-Lavigne, M., Chedotal, A. and Ghosh, A. (2002). Regulation of cortical dendrite development by Slit-Robo interactions. *Neuron* **33**, 47-61.

Wilkinson, D. (1992). Whole mount in situ hybridization of vertebrate embryos. In In Situ *Hybridization: A Practical Approach* (ed. D. G. Wilkinson), pp, 75-83. IRL Press, Oxford.

Wu, W., Wong, K., Chen, J., Jiang, Z., Dupuis, S., Wu, J. Y. and Rao, Y. (1999). Directional guidance of neuronal migration in the olfactory system by the protein Slit. *Nature* **400**, 331-336.

Xian, J., Clark, K. J., Fordham, R., Pannell, R., Rabbitts, T. H. and Rabbitts, P. H. (2001). Inadequate lung development and bronchial hyperplasia in mice with a targeted deletion in the Dutt1/Robo1 gene. *Proc. Natl. Acad. Sci. USA* **98**, 15062-15066.

Yozu, M., Tabata, H. and Nakajima, K. (2005). The caudal migratory stream: a novel migratory stream of interneurons derived from the caudal ganglionic eminence in the developing mouse forebrain. *J. Neurosci.* **25**, 7268-7277.

Yuan, W., Zhou, L., Chen, J. H., Wu, J. Y., Rao, Y. and Ornitz, D. M. (1999). The mouse SLIT family: secreted ligands for ROBO expressed in patterns that suggest a role in morphogenesis and axon guidance. *Dev. Biol.* **212**, 290-306.

Zhang, J., Richards, L. J., Yarowsky, P., Huang, H., van Zijl, P. C. and Mori, S. (2003). Three-dimensional anatomical characterization of the developing mouse brain by diffusion tensor microimaging. *Neuroimage* **20**, 1639-1648.

Zhu, Y., Li, H., Zhou, L., Wu, J. Y. and Rao, Y. (1999). Cellular and molecular guidance of GABAergic neuronal migration from an extracortical origin to the neocortex. *Neuron* **23**, 473-485.

Zou, Y., Stoeckli, E., Chen, H. and Tessier-Lavigne, M. (2000). Squeezing axons out of the gray matter: a role for slit and semaphorin proteins from midline and ventral spinal cord. *Cell* **102**, 363-375.